

# End-to-End Learning of Energy-Constrained Deep Neural Networks

Haichuan Yang<sup>1</sup>, Yuhao Zhu<sup>1</sup>, and Ji Liu<sup>2,1</sup>

<sup>1</sup>University of Rochester, Rochester, USA

<sup>2</sup>Tencent AI Lab, Seattle, USA

`h.yang@rochester.edu, yzhu@rochester.edu, ji.liu.uwisc@gmail.com`

April 18, 2022

## Abstract

Deep Neural Networks (DNN) are increasingly deployed in highly energy-constrained environments such as autonomous drones and wearable devices while at the same time must operate in real-time. Therefore, reducing the energy consumption has become a major design consideration in DNN training. This paper proposes the first end-to-end DNN training framework that provides quantitative energy guarantees. The key idea is to formulate the DNN training as an optimization problem in which the energy budget imposes a previously unconsidered optimization constraint. We integrate the quantitative DNN energy estimation into the DNN training process to assist the constraint optimization. We prove that an approximate algorithm can be used to efficiently solve the optimization problem. Compared to the best prior energy-saving techniques, our framework trains DNNs that provide higher accuracies under same or lower energy budgets.

## 1 Introduction

Deep neural networks (DNN) have become the fundamental building blocks of many emerging application domains such as computer vision [21, 29], speech recognition [17], and natural language processing [11]. Many of these applications have to operate in highly energy-constrained environments. For instance, autonomous drones have to continuously perform computer vision tasks (e.g., object detection) without a constant power supply. Designing DNNs that can meet severe energy budgets has increasingly become a major design objective.

Traditionally, energy consumption of DNNs has been addressed only indirectly through techniques such as pruning [14, 26, 34, 25, 31] and quantization [12, 32, 14, 7, 28] that reduce the DNN model complexity. These techniques are agonistic to energy consumption; rather they are designed to reduce the amount of computations and the amount of model parameters in a DNN, which indirectly reduces the total energy consumption. Recently, energy-aware pruning [33] proposes to directly reduce the energy consumption of DNN inferences by guiding weight pruning using DNN energy estimations. It has demonstrated higher energy savings compared to the indirect, energy-agnostic techniques.

All the existing energy-optimizing methods suffer from two major limitations. First, existing methods usually use various heuristics such as selectively restoring pruned weights and layer by layer

fine-tuning [15, 33]. These heuristics are effective in practice but also have many hyper-parameters that must be carefully tuned. In contrast, we would prefer an *end-to-end* approach that can train an DNN model that is inherently energy-efficient. Second, all existing approaches cannot provide *quantitative energy guarantees*. Specifically, energy-agnostic pruning and quantization do not provide any energy guarantees at all; energy-aware pruning achieves better energy reduction under the same accuracy threshold, but cannot guarantee that the energy consumption is below a particular budget.

In this paper, we aspire to answer the following key question: *can we design DNN models that satisfy a given energy budget while maximizing the accuracy?* This work provides a positive answer to this question through an end-to-end training framework. The key idea is to formulate the DNN training process as an optimization problem in which the energy budget imposes a previously unconsidered optimization constraint. We integrate the quantitative DNN energy estimation into the DNN training process to assist the constraint optimization. In this way, a DNN model, once is trained, by design meets the energy budget while maximizing the accuracy.

Without losing generality, we model the DNN energy consumption after the popular systolic array hardware architecture that is increasingly adopted in today’s DNN hardware chips such as Google’s Tensor Processing Unit (TPU) [19]. The systolic array architecture embodies key design principles of many DNN-specific hardware architectures. Thus, our energy modeling can be extended to support other forms of DNN hardware chips [5, 13]. We specifically focus on pruning, i.e., controlling the DNN sparsity, as the main energy reduction technique. Overall, the energy model models the DNN inference energy as a function of the sparsity of the layer parameters and the layer input.

Given the DNN energy estimation, we formulate the DNN training process as an optimization problem that minimizes the accuracy loss under the constraint of a certain energy budget. The key difference between our optimization formulation and the formulation in a conventional DNN training is two-fold. First, our optimization problem considers the energy constraint, which is not present in conventional training. Second, layer inputs are non-trainable parameters in conventional DNN training since they depend on the initial network input. We introduce a new concept, called input mask, that enables the input sparsity to be a trainable parameter, and thus increases the energy reduction opportunities. This let us further reduce energy in scenarios where the input data pattern is regular.

We propose an optimization algorithm to approximately solve the above optimization problem. A key step in optimization is the projection operation onto the energy constraint. We prove that this projection can be casted into a 0/1 knapsack problem and show that it can be solved very efficiently. Evaluation results show that the our proposed training framework can achieve higher accuracy under the same or lower energy compared to the state-of-the-art energy-saving methods.

In summary, we make the following contributions in this paper:

- To the best of our knowledge, this is the first end-to-end DNN training framework that provides quantitative energy guarantees;
- We propose a quantitative model to estimate the energy consumption of DNN inference on TPU-like hardware. The model can be extended to model other forms of DNN hardware;
- We formulate a new optimization problem for energy-constrained DNN training and present a general optimization algorithm that solves the problem.

## 2 Related Work

**Energy-Agnostic Optimizations** Most existing DNN optimizations indirectly optimize DNN energy through reducing the model complexity. They are agnostic to the energy consumption, and therefore cannot provide any quantitative energy guarantees.

Pruning, otherwise known as sparsification, is perhaps the most widely used technique to reduce DNN model complexity by reducing computation as well as hardware memory access. It is based on the intuition that DNN model parameters that have low-magnitude have little impact on the final prediction, and thus can be zeroed-out. The classic magnitude-based pruning [15] removes weights whose magnitudes are lower than a threshold. Subsequent work guides pruning using special structures [26, 34, 25, 31], such as removing an entire channel, to better retain accuracy after pruning.

Quantization reduces the number of bits used to encode model parameters, and thus reducing computation energy and data access energy [12, 32, 14]. The extreme case of quantization is using 1-bit to represent model parameters [7, 28]. Such binary quantization methods are usually trained from scratch instead of quantizing a pre-trained DNN.

There are other techniques such as low-rank factorization [23, 10, 30] and knowledge distillation [1] that also indirectly affect DNN energy. Low-rank factorization uses tensor/matrix decomposition methods to decompose DNN model parameters. It reduces the number of parameters and simplifies computation. Knowledge distillation uses a smaller model to approximate the output of a large model. Neither technique provides any energy guarantees.

**Energy-Aware Optimizations** Recently, energy-aware pruning (EAP) [33] proposes to use a quantitative energy model to guide model pruning. Different from pure magnitude-based pruning methods, EAP selectively prunes the DNN layer that contributes the most to the total energy consumption. It then applies a sequence of fine-tuning techniques to retain model accuracy. The pruning step and fine-tuning step are alternated until the accuracy loss exceeds a given threshold.

Although EAP a promising first-step toward energy-aware optimizations, its key limitation is that it does not provide quantitative energy guarantees because it does not explicitly consider energy budget as a constraint. Our work integrates the energy budget as an optimization constraint in model training.

## 3 Modeling DNN Inference Energy Consumption

This section introduces the model of estimating energy consumption of a single DNN inference. We consider the widely-used feed-forward DNNs. Note that our proposed methodology is not limited to a particular DNN model or architecture; rather, the principal idea can be easily extended to other network architectures, e.g. recurrent neural networks, as well.

In this section, we first provide an overview of our energy modeling methodology (Section 3.1). We then present the detailed per-layer energy modeling (Section 3.2 and Section 3.3), which allow us to then derive the overall DNN energy consumption (Section 3.4).

### 3.1 Energy Modeling Overview

A DNN typically consists of a sequence of convolution (CONV) layers and fully connected (FC) layers interleaved with a few other layer types such as Rectified Linear Unit (ReLU) and batch normalization. We focus mainly on modeling the energy consumption of the CONV and FC layers.

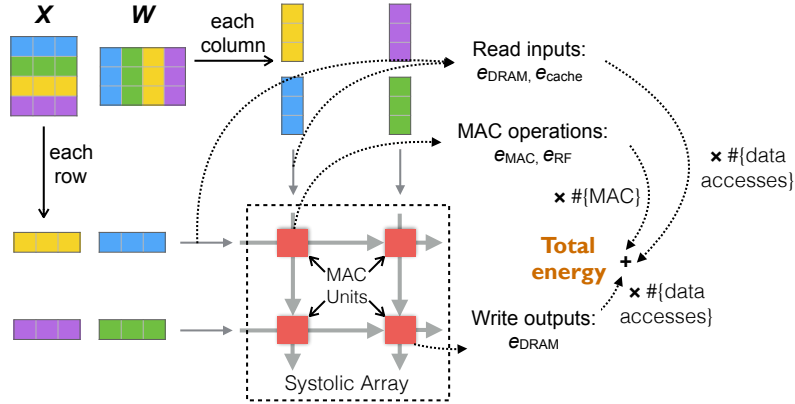


Figure 1: Illustration of the energy cost of computing matrix multiplication  $XW$ .

This is because CONV and FC layers comprise more than 90% of the total execution time during a DNN inference [5] and are the major energy consumers [14, 33]. Energy consumed by other layer types is insignificant and can be taken away from the energy budget as a constant factor.

A DNN inference’s energy consumption is necessarily tied to the underlying hardware where the inference is performed. Without losing generality, we assume a systolic-array-based hardware architecture. Systolic arrays [22] have long been known as effective yet simple designs for matrix multiplication. Many DNN hardware architectures adopt the systolic array, most notably the Google Tensor Processing Unit (TPU) [19].

Figure 1 shows the overall hardware architecture. The systolic array comprises of several compute units that perform the Multiply-and-Accumulate (MAC) operation, which conducts the following computation:  $a \leftarrow a + (b \times c)$ , where  $b$  and  $c$  are the two scalar inputs and  $a$  is the scalar intermediate result called “partial sum.” MAC operation is the building block for matrix multiplication. The MAC units are organized in a 2-D fashion. The data is fed from the edges, both horizontally and vertically, which then propagate to the MAC units within the same row and columns.

We decompose the energy cost into two parts: computation energy  $E_{\text{comp}}$  and data access energy  $E_{\text{data}}$ .  $E_{\text{comp}}$  denotes the energy consumed by computation units, and  $E_{\text{data}}$  denotes the energy consumed when accessing data from the hardware memory. Since we mainly use pruning as the energy reduction technique, we now model how  $E_{\text{comp}}$  and  $E_{\text{data}}$  are affected by DNN sparsity.

### 3.2 Energy Consumption for Computation

CONV layers perform convolution and FC layer perform matrix-vector multiplication. Both operations can be generalized to matrix-matrix multiplication, which involves only the MAC operation [6, 19]. Figure 1 illustrates how a matrix-matrix multiplication is carried out on the systolic array hardware. Given  $X$  and  $W$ , the systolic array computes  $XW$  by passing each row of  $X$  to each row in the systolic array and passing each column of  $W$  to each column in the systolic array. If the width of the systolic array, denoted by  $s_w$ , is less than the width of  $W$ , the hardware will fold  $W$  column-wise in strides of  $s_w$ . Similarly, if the height of  $X$  is greater than the height of the systolic array ( $s_h$ ),  $X$  is folded row-wise in strides of  $s_h$ . Figure 1 illustrates a  $2 \times 2$  systolic array multiplying two  $4 \times 4$  matrices. Both matrices are folded twice in strides of 2.

Critically, if either inputs of a MAC operation is zero, we can skip the MAC operation entirely

and thus save the computation energy. At a high-level, the total computation energy,  $E_{\text{comp}}$ , can be modeled as  $e_{\text{MAC}}N_{\text{MAC}}$ , where  $e_{\text{MAC}}$  denotes the energy consumption of one MAC operation whereas  $N_{\text{MAC}}$  denotes the total number of MAC operations that are actually performed. The challenge is to identify  $N_{\text{MAC}}$  for CONV and FC layers, which we discuss below.

**Fully connected layer** Let  $X^{(v)} \in \mathbb{R}^c$  be the input vector and  $W^{(v)} \in \mathbb{R}^{c \times d}$  be the weight matrix of the FC layer  $v$ . The FC layer performs matrix-vector multiplication  $X^{(v)}W^{(v)}$ . Theoretically, sparsity in both  $X^{(v)}$  and  $W^{(v)}$  will affect  $N_{\text{MAC}}$ . In practice, we consider only the sparsity of  $W^{(v)}$ . This is because the sparsity of  $X^{(v)}$  depends on input (e.g., the content of an image), and is thus non-deterministic at training time. Therefore,  $N_{\text{MAC}} = \|W^{(v)}\|_0$ , and for a fully connected layer  $v$ :

$$E_{\text{comp}}^{(v)} = e_{\text{MAC}}\|W^{(v)}\|_0. \quad (1)$$

**Convolution layer** The CONV layer performs the convolution operation between a 4-D weight (also referred to as kernel or filter) tensor and a 3-D input tensor. Let  $W^{(u)} \in \mathbb{R}^{d \times c \times r \times r}$  be the weight tensor, where  $d$ ,  $c$ , and  $r$  are tensor dimension parameters. Let  $X^{(u)} \in \mathbb{R}^{c \times h \times w}$  be the input tensor, where  $h$  and  $w$  are the input height and width. The convolution operation in the CONV layer  $u$  generates a 3-dimensional tensor:

$$(X^{(u)} * W^{(u)})_{j,x,y} = \sum_{i=1}^c \sum_{r',r''=0}^{r-1} X_{i,x+r',y+r''}^{(u)} W_{j,i,r',r''}^{(u)} \quad (2)$$

Tensor convolutions are often converted to matrix-matrix multiplication for computation efficiency reasons [3]. Specifically, we would unfold the tensor  $X^{(u)}$  to a matrix  $\bar{X}^{(u)} \in \mathbb{R}^{\frac{hw}{s^2} \times cr^2}$ , and unfold the tensor  $W^{(u)}$  to a matrix  $\bar{W}^{(u)} \in \mathbb{R}^{cr^2 \times d}$ , where  $s$  is the convolution stride.  $\bar{X}^{(u)}$  and  $\bar{W}^{(u)}$  are then multiplied together in the systolic array to compute the equivalent convolution result between  $X^{(u)}$  and  $W^{(u)}$ .

Nonzero elements in  $W^{(u)}$  incur actual MAC operations. Thus,  $N_{\text{MAC}} = \|W^{(u)}\|_0 hw/s^2$ , resulting in the following computation energy of a CONV layer  $u$ :

$$E_{\text{comp}}^{(u)} = (e_{\text{MAC}}hw/s^2)\|W^{(u)}\|_0. \quad (3)$$

### 3.3 Energy Consumption for Data Access

Accessing data happens in every layer. The challenge in modeling the data access energy is that modern hardware is equipped with a multi-level memory hierarchy in order to improve speed and save energy [16]. Specifically, the data is originally stored in a large memory, which is slow and energy-hungry. When the data is needed to perform certain computation, the hardware will load it from the large memory into a smaller memory that is faster and consume less energy. If the data is reused often, it will mostly live in the small memory. Thus, such a multi-level memory hierarchy saves overall energy and improves overall speed by exploiting data reuse.

Without losing generality, we model a three-level memory hierarchy composed of a Dynamic Random Access Memory (DRAM), a Cache, and a Register File (RF). The cache is split into two halves: one for holding  $X$  (i.e., the feature map in a CONV layer and the feature vector in a FC layer) and the other for holding  $W$  (i.e., the convolution kernel in a CONV layer and the weight matrix in an FC layer). This is by far the most common memory hierarchy in DNN hardware such as Google’s TPU [19, 5, 35, 13]. Data is always loaded from DRAM into cache, and then from cache

to RFs. Critically, if the value of the data that is being loaded is zero, the hardware can skip the data access and thereby save energy.

To compute  $E_{\text{data}}$ , we must calculate the number of data accesses at each memory level, i.e.,  $N_{\text{DRAM}}, N_{\text{cache}}, N_{\text{RF}}$ . Let the unit energy costs of different memory hierarchies be  $e_{\text{DRAM}}, e_{\text{cache}}$ , and  $e_{\text{RF}}$ , respectively, the total data access energy consumption  $E_{\text{data}}$  will be  $e_{\text{DRAM}}N_{\text{DRAM}} + e_{\text{cache}}N_{\text{cache}} + e_{\text{RF}}N_{\text{RF}}$ . We now derive the detailed data access energy in FC and CONV layers.

**Fully connected layer** To multiply  $X^{(v)} \in \mathbb{R}^c$  and  $W^{(v)} \in \mathbb{R}^{c \times d}$ , each nonzero element of  $W^{(v)}$  is used once but loaded three times, once each from DRAM, cache and RF, respectively. Thus, the number of DRAM, cache, and RF accesses for weight matrix  $X^{(v)}$  is:

$$N_{\text{DRAM}}^{\text{weights}} = N_{\text{cache}}^{\text{weights}} = N_{\text{RF}}^{\text{weights}} = \|W^{(v)}\|_0. \quad (4)$$

Input  $X^{(v)}$  is fed into the systolic array  $\lceil d/s_w \rceil$  times, where  $s_w$  denotes the the systolic array width. Thus, the number of cache accesses for  $X^{(v)}$  is:

$$N_{\text{cache}}^{\text{input}} = \lceil d/s_w \rceil \|X^{(v)}\|_0. \quad (5)$$

Let  $k_X$  be the cache size for input  $X^{(v)}$ . If  $k_X$  is less than  $\|X^{(v)}\|_0$ , there are  $\|X^{(v)}\|_0 - k_X$  elements that must be reloaded from DRAM every time. The rest  $k_X$  elements need to load from DRAM only once as they will always reside in cache. Thus, there are  $\lceil d/s_w \rceil (\|X^{(v)}\|_0 - k_X) + k_X$  DRAM accesses for  $X^{(v)}$ . In addition, the output vector of the FC layer (result of  $X^{(v)}W^{(v)}$ ) needs to be written back to DRAM, which further incurs  $d$  DRAM accesses. Thus, The total number of DRAM accesses to retrieve  $X^{(v)}$  is:

$$N_{\text{DRAM}}^{\text{input}} = \lceil d/s_w \rceil \max(0, \|X^{(v)}\|_0 - k_X) + \min(k_X, \|X^{(v)}\|_0) + d. \quad (6)$$

Each input element is loaded from RF once for each MAC operation, and there are two RF accesses incurred by accumulation for each MAC operation (one read and one write). Thus, the total number of RF accesses related to  $X^{(v)}$  is:

$$N_{\text{RF}}^{\text{input}} = d\|X^{(v)}\|_0 + 2\|W^{(v)}\|_0. \quad (7)$$

In summary, the data access energy of a fully connected layer  $v$  is expressed as follows, in which each component follows the derivations in Equation (4) through Equation (7):

$$E_{\text{data}}^{(v)} = e_{\text{DRAM}}(N_{\text{DRAM}}^{\text{input}} + N_{\text{DRAM}}^{\text{weights}}) + e_{\text{cache}}(N_{\text{cache}}^{\text{input}} + N_{\text{cache}}^{\text{weights}}) + e_{\text{RF}}(N_{\text{RF}}^{\text{input}} + N_{\text{RF}}^{\text{weights}}). \quad (8)$$

**Convolution layer** Similar to a FC layer, the data access energy of a CONV layer  $u$  is modeled as:

$$E_{\text{data}}^{(u)} = e_{\text{DRAM}}(N_{\text{DRAM}}^{\text{input}} + N_{\text{DRAM}}^{\text{weights}}) + e_{\text{cache}}(N_{\text{cache}}^{\text{input}} + N_{\text{cache}}^{\text{weights}}) + e_{\text{RF}}(N_{\text{RF}}^{\text{input}} + N_{\text{RF}}^{\text{weights}}). \quad (9)$$

The notations are the same as in FC layer. We now show how the different components are modeled.

To convolve  $W^{(u)} \in \mathbb{R}^{d \times c \times r \times r}$  with  $X^{(u)} \in \mathbb{R}^{c \times h \times w}$ , each nonzero element in the weight tensor  $W^{(u)}$  is fed into the systolic array  $\lceil (hw/s^2)/s_h \rceil$  times, where  $s_h$  denotes the height of the systolic array. Thus,

$$N_{\text{cache}}^{\text{weights}} = \lceil (hw/s^2)/s_h \rceil \|W^{(u)}\|_0. \quad (10)$$

Similarly to the FC layer, the number of RF accesses for  $W^{(u)}$  during all the MAC operations is:

$$N_{\text{RF}}^{\text{weights}} = \lceil (hw/s^2) \rceil \|W^{(u)}\|_0. \quad (11)$$

Let  $k_W$  be the cache size for the weight matrix  $W^{(u)}$ . If  $\|W^{(u)}\|_0 > k_W$ , there are  $k_W$  nonzero elements of  $W^{(u)}$  that would be accessed from DRAM only once as they would reside in the cache, and the rest  $\|W^{(u)}\|_0 - k_W$  elements would be accessed from DRAM by  $\lceil (hw/s^2)/s_h \rceil$  times. Thus,

$$N_{\text{DRAM}}^{\text{weights}} = \lceil (hw/s^2)/s_h \rceil \max(0, \|W^{(u)}\|_0 - k_W) + \min(k_W, \|W^{(u)}\|_0). \quad (12)$$

Let  $k_X$  be the cache size for input  $X^{(u)}$ . If every nonzero element in  $X^{(u)}$  is loaded from DRAM to cache only once,  $N_{\text{DRAM}}^{\text{input}}$  would simply be  $\|X^{(u)}\|_0$ . In practice, however, the cache size  $k_X$  is much smaller than  $\|X^{(u)}\|_0$ . Therefore, some portion of  $X^{(u)}$  would need to be re-loaded. To calculate the amount of re-loaded DRAM access, we observe that in real hardware  $X^{(u)}$  is loaded from DRAM to the cache at a row-granularity (i.e., at least  $cw$  elements are loaded at once). In this way, the cache would first load  $\lfloor k_X/(cw) \rfloor$  rows from DRAM, and after the convolutions related to these rows have finished, the cache would load the next  $\lfloor k_X/(cw) \rfloor$  rows in  $X^{(u)}$  for further processing.

The rows loaded in the above two rounds have overlaps due to the natural of the convolution operation. The exact number of overlaps  $R_{\text{overlap}}$  is  $\lceil h/(\lfloor k_X/cw \rfloor - r + s) \rceil - 1$ , and each overlap has  $cw(r - s)$  elements. Thus,  $R_{\text{overlap}} \times cw(r - s)$  elements would need to be reloaded from DRAM. Finally, storing the outputs of the convolution incurs an additional  $d(hw/s^2)$  DRAM writes. Summing the different parts together, the number of DRAM accesses for  $X$  is:

$$N_{\text{DRAM}}^{\text{input}} = \|X^{(u)}\|_0 + (\lceil h/(\lfloor k_X/cw \rfloor - r + s) \rceil - 1)cw(r - s) + d(hw/s^2). \quad (13)$$

Every nonzero element in  $X$  would be fed into the systolic array  $\lceil d/s_w \rceil r^2/s^2$  times. Each MAC operation introduce 2 RF accesses. Thus,

$$N_{\text{cache}}^{\text{input}} = (\lceil d/s_w \rceil r^2/s^2) \|X^{(u)}\|_0, \quad N_{\text{RF}}^{\text{input}} = (dr^2/s^2) \|X^{(u)}\|_0 + 2(hw/s^2) \|W^{(u)}\|_0. \quad (14)$$

### 3.4 The Overall Energy Estimation Formulation

Let  $U$  and  $V$  be the sets of convolutional layers and fully connected layers in a DNN respectively. The subscript  $^{(u)}$  and  $^{(v)}$  indicate the energy consumption of layer  $u \in U$  and  $v \in V$ , respectively. Then the overall energy consumption of a DNN inference can be modeled by

$$E(X, W) := \sum_{u \in U} (E_{\text{comp}}^{(u)} + E_{\text{data}}^{(u)}) + \sum_{v \in V} (E_{\text{comp}}^{(v)} + E_{\text{data}}^{(v)}) \quad (15)$$

where  $X$  stacks input vectors/tensors at all layers and  $W$  stacks weight matrices/tensors at all layers.

## 4 Energy Constrained DNN Model

Given the energy model presented in Section 3, we propose a new energy-constrained DNN model that bounds the energy consumption of a DNN's inference. This section formulates its training as an optimization problem. We first formulate the optimization constraint by introducing a trainable mask variable into the energy modeling to enforce layer input sparsity. We then define a new loss function

by introducing the knowledge distillation regularizer that helps improve training convergence and reduce overfitting.

**Controlling Input Sparsity Using Input Mask** The objective of training an energy-constrained DNN is to minimize the accuracy loss while ensuring that the DNN inference energy is below a given budget,  $E_{\text{budget}}$ . Since the total energy consumption is a function of  $\|X^{(u)}\|_0$  and  $\|W^{(u)}\|_0$ , it is natural to think that the trainable parameters are  $X$  and  $W$ . In reality, however,  $X$  depends on the input to the DNN (e.g., an input image to an object recognition DNN), and thus is unknown during training time. Therefore, in conventional DNN training frameworks  $X$  is never trainable.

To include the sparsity of  $X$  in our training framework, we introduce a trainable binary mask  $M$  that is of the same shape of  $X$ , and is multiplied with  $X$  before  $X$  is fed into CONV or FC layers, or equivalently, at the end of the previous layer. For example, if the input to a standard CONV layer is  $X^{(u)}$ , the input would now be  $X^{(u)} \odot M^{(u)}$ , where  $\odot$  denotes the element-wise multiplication.

With the trainable mask  $M$ , we can ensure that  $\|X^{(u)} \odot M^{(u)}\|_0 \leq \|M^{(u)}\|_0$ , and thereby control the sparsity of the input at training time. In this way, the optimization constraint of our training framework becomes  $E(M, W) \leq E_{\text{budget}}$ , where  $E(M, W)$  denotes the total DNN inference energy consumption, which is a function of  $X$  and  $W$  (as shown in Equation (15)), and thus a function of  $M$  and  $W$ .

**Knowledge Distillation as a Regularizer** Directly optimizing over the constraint would likely lead to a local optimum because the energy model is highly non-convex. To improve the training performance, we apply the knowledge distillation loss [1] as a regularization to the conventional loss function. Intuitively, the regularization uses a pre-trained dense model to guide the training of a sparse model. Specifically, our regularized loss function is:

$$\bar{\mathcal{L}}_{\lambda, W_{\text{dense}}}(M, W) := \mathcal{L}(M, W) + \lambda \mathbb{E}_X [\|\phi(X; W) - \phi(X; W_{\text{dense}})\|^2], \quad (16)$$

where  $W_{\text{dense}}$  is the original dense model,  $\phi(X; W)$  is the network’s output (we use the output before the last activation layer as in [1]), and  $\lambda$  is a hyper parameter similar to other standard regularizations.

Thus, training an energy-constrained DNN model is formulated as an optimization problem:

$$\min_{M, W} \bar{\mathcal{L}}_{\lambda, W_{\text{dense}}}(M, W) \quad \text{s.t.} \quad E(M, W) \leq E_{\text{budget}}. \quad (17)$$

## 5 Optimization

This section introduces an algorithm to solve the optimization problem formulated in (17). The overall algorithm is shown in Algorithm 1. Specifically, the algorithm includes three key parts:

- Initialization by training a dense model. That is,

$$W_{\text{dense}} := \arg \min_W \mathcal{L}(M, W) \quad (18)$$

- Fix  $M$  and optimize  $W$  via approximately solving (using  $W_{\text{dense}}$  initialization):

$$\min_W \bar{\mathcal{L}}(M, W) \quad \text{s.t.} \quad E(M, W) \leq E_{\text{budget}} \quad (19)$$



---

**Algorithm 1:** Energy-Constrained DNN Training.

---

**Input:** Energy budget  $E_{\text{budget}}$ , learning rates  $\eta_1, \eta_2$ , mask sparsity decay step  $\Delta q$ .  
**Result:** DNN weights  $W^*$ , input mask  $M^*$ .

- 1 Initialize  $W = W_{\text{dense}}, M = \mathbf{1}, q = \|M\|_0 - \Delta q$ ;
- 2 **while** *True* **do**
  - // Update DNN weights*
  - 3 **while** *W has not converged* **do**
    - 4  $W = W - \eta_1 \hat{\nabla}_W \bar{\mathcal{L}}(M, W)$ ; *// SGD step*
    - 5  $W = P_{\Omega(E_{\text{budget}})}(W)$ ; *// Energy constraint projection for weights W*
  - 6 **end**
  - 7 If *previous\_accuracy > current\_accuracy*, exit loop with previous  $W$  and  $M$ ;
  - // Update input mask*
  - 8 **while** *M has not converged* **do**
    - 9  $M = M - \eta_2 \hat{\nabla}_M \bar{\mathcal{L}}(M, W)$ ; *// SGD step*
    - 10 Clamp values of  $M$  into  $[0, 1]$ : assign 1 (or 0) to the values if they exceeds 1 (or negative);
    - 11  $M = P_{\|M\|_0 \leq q}(M)$ ; *// L<sub>0</sub> constraint projection for input mask M*
  - 12 **end**
  - 13 Round values of  $M$  into  $\{0, 1\}$ ;
  - 14 Decay the sparsity constraint  $q = q - \Delta q$ ;
- 15 **end**
- 16  $W^* = W, M^* = M$ .

---

- Fix  $W$  and optimize  $M$  by approximately solving :

$$\min_M \bar{\mathcal{L}}(M, W) \quad \text{s.t.} \quad \|M\|_0 \leq q, M \in [\mathbf{0}, \mathbf{1}] \quad (20)$$

After the initialization step (Line 1 in Algorithm 1), the training algorithm iteratively alternates between the second (Line 3-6 in Algorithm 1) and the third step (Line 8-13 in Algorithm 1) while gradually reducing the sparsity constraint  $q$  (Line 14 in Algorithm 1) until the training accuracy converges. Note that Equation (18) is the classic DNN training process, and solving Equation (20) involves only the well-known  $L_0$  norm projection  $P_{\|M\|_0 \leq q}(Q) := \arg \min_{\|M\|_0 \leq q} \|M - Q\|^2$ . We thus focus on how Equation (19) is solved.

**Optimizing Weight Matrix  $W$**  To solve (19), one can use either projected gradient descent or projected stochastic gradient descent. The key difficulty in optimization lies on the projection step

$$P_{\Omega(E_{\text{budget}})}(Z) := \arg \min_{W \in \Omega(E_{\text{budget}})} \|W - Z\|^2 \quad (21)$$

where  $Z$  could be  $W - \eta \nabla_W \bar{\mathcal{L}}(W, M)$  or replacing  $\nabla_W \bar{\mathcal{L}}(W, M)$  by a stochastic gradient  $\hat{\nabla}_W \bar{\mathcal{L}}(W, M)$ . To solve the projection step, let us take a closer look at the constraint Equation (15). We rearrange the energy constraint  $\Omega(E_{\text{budget}})$  into the following form with respect to  $W$ :

$$\left\{ W \mid \sum_{u \in U \cup V} \alpha_1^{(u)} \min(k, \|W^{(u)}\|_0) + \alpha_2^{(u)} \max(0, \|W^{(u)}\|_0 - k) + \alpha_3^{(u)} \|W^{(u)}\|_0 + \alpha_4^{(u)} \leq E_{\text{budget}} \right\}, \quad (22)$$

where  $W$  stacks all the variable  $\{W^{(u)}\}_{u \in U \cup V}$ , and  $\alpha_1^{(u)}, \alpha_2^{(u)}, \alpha_3^{(u)}, \alpha_4^{(u)}$  and  $k$  are properly defined nonnegative constants. Note that  $\alpha_1^{(u)} \leq \alpha_2^{(u)}$  and  $k$  is a positive integer.

**Theorem 1.** *The projection problem in (21) is equivalent to solving the following 0/1 knapsack problem:*

$$\max_{\xi \text{ is binary}} \langle Z \odot Z, \xi \rangle, \quad \text{s.t.} \quad \langle A, \xi \rangle \leq E_{\text{budget}} - \sum_{u \in U \cup V} \alpha_4^{(u)}, \quad (23)$$

where  $Z$  stacks all the variables  $\{Z^{(u)}\}_{u \in U \cup V}$ ,  $A$  and  $\xi$  are of the same shape as  $Z$ , and the  $j$ -th element of  $A^{(u)}$  for any  $u \in U \cup V$  is defined by

$$A_j^{(u)} = \begin{cases} \alpha_1^{(u)} + \alpha_3^{(u)}, & \text{if } Z_j^{(u)} \text{ is among the top } k \text{ elements of } Z^{(u)} \text{ in term of magnitude;} \\ \alpha_2^{(u)} + \alpha_3^{(u)}, & \text{otherwise.} \end{cases} \quad (24)$$

The optimal solution of (21) is  $Z \odot \xi^*$ , where  $\xi^*$  is the optimal solution to the knapsack problem (23).

The knapsack problem is NP hard. But it is possible to find an approximate solution efficiently. There exist approximate algorithms [2] that can find an  $\epsilon$ -accurate solution in  $O(n \log(1/\epsilon) + \epsilon^{-2.4})$  computational complexity. However, due to some special structure in our problem, there exists an algorithm that can find an  $\epsilon$ -accurate solution much faster.

**Theorem 2.** *For the projection problem (21), there exists an efficient approximation algorithm with  $O\left(\left(n + \frac{(|U|+|V|)^3}{\epsilon^2}\right) \log \frac{n \max(A)}{\min(A_+)}\right)$  computational complexity outputting a solution  $W' \in \Omega(E_{\text{budget}})$  that admits*

$$\|W' - Z\|^2 \leq \left\| P_{\Omega\left(\frac{E_{\text{budget}}}{1+O(\epsilon)}\right)}(Z) - Z \right\|^2, \quad (25)$$

where  $\min(A_+)$  is the minimum of the positive elements in  $A$ .

In our case,  $|U|$  and  $|V|$  denote the numbers of convolutional layers and fully connected layers, respectively. They are very small numbers that can be treated as constants here. Therefore, the computational complexity for our problem can be reduced to  $\tilde{O}(n + \frac{1}{\epsilon^2})$ , where  $\tilde{O}$  omits the logarithm term.

The implementation of the algorithm in Theorem 2 is very complicated. Alternatively, we propose to run a simple but efficient approximate algorithm based on the ‘‘profit density’’ (the profit density of item  $j$  is defined by  $Z_j^2/A_j$ ). We sort all items based on the ‘‘profit density’’ and select a group of largest items until reach the constraint boundary. The detailed algorithm description is shown in Algorithm 2, and such greedy approximation algorithm also admits nice property as shown in Theorem 3.

**Theorem 3.** *For the projection problem (21), the approximate solution  $W'' \in \Omega(E_{\text{budget}})$  to the greedy approximation algorithm described in Algorithm 2 admits*

$$\|W'' - Z\|^2 \leq \|P_{\Omega(E_{\text{budget}})}(Z) - Z\|^2 + \text{Top}_{\|W''\|_0+1}((Z \odot Z) \oslash A) \cdot \min((\max(A) - \text{gcd}(A)), R(W'')) \quad (26)$$

where  $\max(A)$  is the maximal element of  $A$ ,  $A$  is a nonnegative matrix defined in (24),  $\text{Top}_k(\cdot)$  returns the  $k$ -th largest element of  $\cdot$ ,  $\oslash$  denotes the element-wise division. We define  $\text{gcd}(\cdot)$  as the

---

**Algorithm 2:** Greedy Algorithm to Solve Problem (23).

---

**Input:**  $Z, A, E_{\text{budget}}, \{\alpha^{(u)}\}_{u \in U \cup V}$  as in (23).

**Result:** Greedy solution  $\tilde{\xi}$  for problem (23).

- 1 Initialize  $b = 0, \xi = \mathbf{0}$ .
- 2 Generate the profit density  $\delta$ :

$$\delta_j = \begin{cases} (Z_j)^2/A_j, & \text{if } A_j > 0; \\ \infty, & \text{if } A_j = 0. \end{cases}$$

- 3 Sort  $\delta$ , let  $I$  be the indices list of the sorted  $\delta$  (in descending order).
  - 4 **foreach** index  $j \in I$  **do**
  - 5      $b = b + A_j$ ;
  - 6     If  $b > E_{\text{budget}} - \sum_{u \in U \cup V} \alpha_4^{(u)}$ , exit loop;
  - 7      $\xi_j = 1$ ;
  - 8 **end**
  - 9  $\tilde{\xi} = \xi$ .
- 

largest positive rational number that divides each of the arguments, e.g.,  $\text{gcd}(0, 1/3, 2/3) = 1/3$ . In (26),  $\text{gcd}(A)$  denotes the greatest common divisor of all elements in  $A$ , and  $R(W'')$  denotes the remaining budget

$$R(W'') = \left( E_{\text{budget}} - \sum_{u \in U \cup V} \alpha_4^{(u)} - \langle A, \text{supp}(W'') \rangle \right),$$

where  $\text{supp}(W'')$  is binary and it indicates the nonzero elements of  $W''$ .

We can see that  $W''$  is the optimal projection solution to (21) if either of the following two conditions holds:

1. (**The remaining budget is 0.**) It means that the greedy method in Algorithm 2 runs out of all budget;
2. (**The matrix  $A$  satisfies  $\max(A) = \text{gcd}(A)$ .)** It implies that all elements in  $A$  are either 0 or a certain constant. In other words, the weights for all items are either zero or identical.

## 6 Evaluation

We compare our method with three state-of-art pruning methods: magnitude-based pruning (MP) [15, 14], structured sparsity learning (SSL) [31], and energy-aware pruning (EAP) [33]. We evaluate on ImageNet [9], MNIST, and VGG-Face datasets [27]. We use both classic DNNs, including AlexNet [21] and LeNet-5 [24], as well as recently proposed SqueezeNet [18] and MobileNetV2 [4] that are purposely-designed to be light-weight.

**Hyper-parameters** For knowledge distillation regularization, we choose a positive  $\lambda = 1/|\phi(X; W)|$  on ImageNet and VGG-Face, where  $|\phi(X; W)|$  is the network output dimensionality. We set  $\lambda = 0$  in MNIST, which has little overfitting issue. In all the experiments, we choose

Table 1: Energy consumption and accuracy drops compared to dense models on ImageNet. We set the energy budget according to the lowest energy consumption obtained from prior art.

DNNs	AlexNet				SqueezeNet				MobileNetV2		
Energy Budget	27%				64%				74%		
Methods	MP	SSL	EAP	Ours	MP	SSL	EAP	Ours	MP	SSL	Ours
Accuracy Drop	0.06%	1.12%	0.87%	<b>0.70%</b>	-0.86%	0.12%	0.14%	<b>0.03%</b>	0.63%	0.73%	<b>0.31%</b>
Energy	47%	51%	27%	<b>27%</b>	87%	64%	76%	<b>64%</b>	75%	74%	<b>74%</b>

$\Delta q = 0.1|M|$  where  $|M|$  is the number of all mask elements. For optimizing  $W$ , we use SGD with a learning rate  $\eta_1 = 0.01$  on AlexNet, LeNet-5, and MobileNetV2, and use  $\eta_1 = 0.001$  on SqueezeNet. For optimizing input mask parameters  $M$ , we use the Adam optimizer [20] with  $\eta_2 = 0.0001$ .

## 6.1 ImageNet

For a fair comparison, we set the energy budget according to the *minimal energy consumption* obtained from the three baseline schemes. We also use the same hardware parameters, i.e.,  $e_{MAC}$ ,  $e_{DRAM}$ ,  $e_{cache}$ ,  $e_{RF}$ ,  $s_h$ ,  $s_w$ ,  $k_W$ ,  $k_X$ , as described in the EAP paper [33].

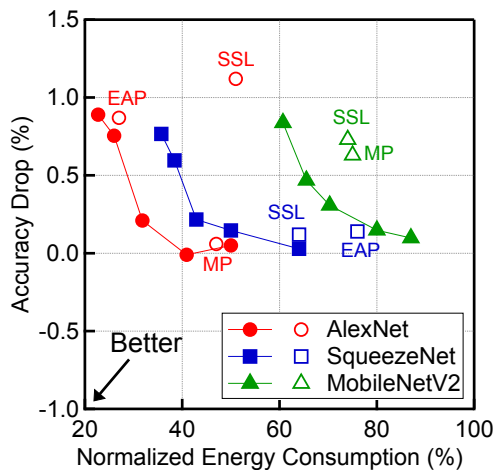


Figure 2: Accuracy drops under different energy consumptions.

Table 1 shows the (top-5 validation) accuracy drop and energy consumption of various techniques compared to the dense model. Our training framework consistently achieves a higher accuracy with a lower energy consumption under the same energy budget. For instance on AlexNet, under the same 27% energy budget, our technique achieves lower accuracy drop over EAP (0.7% vs. 0.87%). The advantage is also evident in SqueezeNet and MobileNetV2 that are already light-weight by design. EAP does not report data on MobileNetV2.

Figure 2 comprehensively compares our technique with prior work. Solid markers represent DNNs trained from our framework under different energy budgets ( $x$ -axis). Empty markers represent DNNs produced from previous techniques. DNNs trained by our techniques generally have lower energies with higher accuracies (i.e., solid markers are closer to the bottom-left corner than empty markers). For instance on SqueezeNet, our most energy-consuming DNN still reduces energy by 13%

Table 2: Energy consumptions and accuracy drops on MNIST and VGG-Face. The energy budget is set according to the lower energy consumption obtained from MP and SSL.

DNNs@Dataset	LeNet-5@MNIST			MobileNetV2@VGG-Face		
Energy Budget	21%			45%		
Methods	MP	SSL	<b>Ours</b>	MP	SSL	<b>Ours</b>
Accuracy Drop	1.51%	2.51%	<b>0.96%</b>	1.78%	1.27%	<b>0.95%</b>
Energy	23%	21%	<b>21%</b>	45%	48%	<b>45%</b>

while improves accuracy by 0.12% compared to EAP, which achieves the the state-of-the-art energy savings.

## 6.2 MNIST and VGG-Face

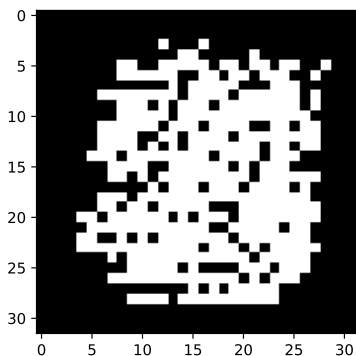


Figure 3: Trained input mask applied to the first layer of LeNet-5 on MNIST.

MNIST and VGG-Face [27] represent datasets where inputs have regular patterns that are amenable to input mask training. For instance, a digit in a MNIST image most likely appears in the middle of the image. In such a scenario, training input masks lets us control the sparsity of the layer inputs and thus further reduce energy than merely pruning model parameters as in conventional methods. We do not claim that applying input mask is a general technique; rather, we intend to demonstrate its effectiveness when applicable.

We compare our technique with MP and SSL using LeNet-5 and MobileNetV2 for the two datasets, respectively. EAP does not report data on these two datasets. Similarly to the evaluation on ImageNet, we set the energy budget the same as the lower energy consumption between MP and SSL for a fair comparison. Table 2 compares the energy consumption and (validation) accuracy drop. Our technique consistently achieves higher accuracy (lower loss) with lower energy under the same energy budget. The effectiveness of input mask is shown in Figure 3, which shows the trained input mask applied to the first DNN layer.

## 7 Conclusion

This paper demonstrates that it is possible to train DNNs with quantitative energy guarantees in an end-to-end fashion. The enabler is an energy model that relates the DNN inference energy to the

DNN parameters. Leveraging the energy model, we augment the conventional DNN training with an energy-constrained optimization process, which minimizes the accuracy loss under the constraint of a given energy budget. Using an efficient algorithm, our training framework generates DNNs with higher accuracies under the same or lower energy budgets compared to prior art.

## References

- [1] Jimmy Ba and Rich Caruana. Do deep nets really need to be deep? In *Advances in neural information processing systems*, pages 2654–2662, 2014.
- [2] Timothy M Chan. Approximation schemes for 0-1 knapsack. In *OASICs-OpenAccess Series in Informatics*, volume 61. Schloss Dagstuhl-Leibniz-Zentrum fuer Informatik, 2018.
- [3] Kumar Chellapilla, Sidd Puri, and Patrice Simard. High performance convolutional neural networks for document processing. In *Tenth International Workshop on Frontiers in Handwriting Recognition*. Suvisoft, 2006.
- [4] Sheng Chen, Yang Liu, Xiang Gao, and Zhen Han. Mobilefacenet: Efficient cnns for accurate real-time face verification on mobile devices. *arXiv preprint arXiv:1804.07573*, 2018.
- [5] Yu-Hsin Chen, Joel Emer, and Vivienne Sze. Eyeriss: A Spatial Architecture for Energy-efficient Dataflow for Convolutional Neural Networks. In *Proc. of ISCA*, 2016.
- [6] Sharan Chetlur, Cliff Woolley, Philippe Vandermersch, Jonathan Cohen, John Tran, Bryan Catanzaro, and Evan Shelhamer. cudnn: Efficient primitives for deep learning. *arXiv preprint arXiv:1410.0759*, 2014.
- [7] Matthieu Courbariaux, Yoshua Bengio, and Jean-Pierre David. Binaryconnect: Training deep neural networks with binary weights during propagations. In *Advances in neural information processing systems*, pages 3123–3131, 2015.
- [8] George B Dantzig. Discrete-variable extremum problems. *Operations research*, 5(2):266–288, 1957.
- [9] Jia Deng, Wei Dong, Richard Socher, Li-Jia Li, Kai Li, and Li Fei-Fei. Imagenet: A large-scale hierarchical image database. In *Computer Vision and Pattern Recognition, 2009. CVPR 2009. IEEE Conference on*, pages 248–255. IEEE, 2009.
- [10] Emily L Denton, Wojciech Zaremba, Joan Bruna, Yann LeCun, and Rob Fergus. Exploiting linear structure within convolutional networks for efficient evaluation. In *Advances in neural information processing systems*, pages 1269–1277, 2014.
- [11] Yoav Goldberg. A primer on neural network models for natural language processing. *Journal of Artificial Intelligence Research*, 57:345–420, 2016.
- [12] Yunchao Gong, Liu Liu, Ming Yang, and Lubomir Bourdev. Compressing deep convolutional networks using vector quantization. *arXiv preprint arXiv:1412.6115*, 2014.
- [13] Song Han, Xingyu Liu, Huizi Mao, Jing Pu, Ardavan Pedram, Mark Horowitz, and William Dally. EIE: Efficient Inference Engine on Compressed Deep Neural Network. In *Proc. of ISCA*, 2016.
- [14] Song Han, Huizi Mao, and William J Dally. Deep compression: Compressing deep neural networks with pruning, trained quantization and huffman coding. *arXiv preprint arXiv:1510.00149*, 2015.
- [15] Song Han, Jeff Pool, John Tran, and William Dally. Learning both weights and connections for efficient neural network. In *Advances in neural information processing systems*, pages 1135–1143, 2015.
- [16] John L Hennessy and David A Patterson. *Computer architecture: a quantitative approach*. Elsevier, 2011.
- [17] Geoffrey Hinton, Li Deng, Dong Yu, George E Dahl, Abdel-rahman Mohamed, Navdeep Jaitly, Andrew Senior, Vincent Vanhoucke, Patrick Nguyen, Tara N Sainath, et al. Deep neural networks for acoustic modeling in speech recognition: The shared views of four research groups. *IEEE Signal Processing Magazine*, 29(6):82–97, 2012.

- [18] Forrest N Iandola, Song Han, Matthew W Moskewicz, Khalid Ashraf, William J Dally, and Kurt Keutzer. Squeezenet: Alexnet-level accuracy with 50x fewer parameters and < 0.5 mb model size. *arXiv preprint arXiv:1602.07360*, 2016.
- [19] Norman P Jouppi, Cliff Young, Nishant Patil, David Patterson, Gaurav Agrawal, Raminder Bajwa, Sarah Bates, Suresh Bhatia, Nan Boden, Al Borchers, et al. In-datacenter performance analysis of a tensor processing unit. In *Proceedings of the 44th Annual International Symposium on Computer Architecture*, pages 1–12. ACM, 2017.
- [20] Diederik P Kingma and Jimmy Ba. Adam: A method for stochastic optimization. *arXiv preprint arXiv:1412.6980*, 2014.
- [21] Alex Krizhevsky, Ilya Sutskever, and Geoffrey E Hinton. Imagenet classification with deep convolutional neural networks. In *Advances in neural information processing systems*, pages 1097–1105, 2012.
- [22] Hsiang-Tsung Kung. Why systolic architectures? *IEEE computer*, 15(1):37–46, 1982.
- [23] Vadim Lebedev, Yaroslav Ganin, Maksim Rakhuba, Ivan Oseledets, and Victor Lempitsky. Speeding-up convolutional neural networks using fine-tuned cp-decomposition. *arXiv preprint arXiv:1412.6553*, 2014.
- [24] Yann LeCun, Léon Bottou, Yoshua Bengio, and Patrick Haffner. Gradient-based learning applied to document recognition. *Proceedings of the IEEE*, 86(11):2278–2324, 1998.
- [25] Hao Li, Asim Kadav, Igor Durdanovic, Hanan Samet, and Hans Peter Graf. Pruning filters for efficient convnets. *arXiv preprint arXiv:1608.08710*, 2016.
- [26] Baoyuan Liu, Min Wang, Hassan Foroosh, Marshall Tappen, and Marianna Pinsky. Sparse convolutional neural networks. In *Proceedings of the IEEE Conference on Computer Vision and Pattern Recognition*, pages 806–814, 2015.
- [27] Omkar M Parkhi, Andrea Vedaldi, Andrew Zisserman, et al. Deep face recognition. In *BMVC*, volume 1, page 6, 2015.
- [28] Mohammad Rastegari, Vicente Ordonez, Joseph Redmon, and Ali Farhadi. Xnor-net: Imagenet classification using binary convolutional neural networks. In *European Conference on Computer Vision*, pages 525–542. Springer, 2016.
- [29] Karen Simonyan and Andrew Zisserman. Very deep convolutional networks for large-scale image recognition. *arXiv preprint arXiv:1409.1556*, 2014.
- [30] Cheng Tai, Tong Xiao, Yi Zhang, Xiaogang Wang, et al. Convolutional neural networks with low-rank regularization. *arXiv preprint arXiv:1511.06067*, 2015.
- [31] Wei Wen, Chunpeng Wu, Yandan Wang, Yiran Chen, and Hai Li. Learning structured sparsity in deep neural networks. In *Advances in Neural Information Processing Systems*, pages 2074–2082, 2016.
- [32] Jiaxiang Wu, Cong Leng, Yuhang Wang, Qinghao Hu, and Jian Cheng. Quantized convolutional neural networks for mobile devices. In *Proceedings of the IEEE Conference on Computer Vision and Pattern Recognition*, pages 4820–4828, 2016.
- [33] Tien-Ju Yang, Yu-Hsin Chen, and Vivienne Sze. Designing energy-efficient convolutional neural networks using energy-aware pruning. In *Proceedings of the IEEE Conference on Computer Vision and Pattern Recognition*, pages 5687–5695, 2017.
- [34] Hao Zhou, Jose M Alvarez, and Fatih Porikli. Less is more: Towards compact cnns. In *European Conference on Computer Vision*, pages 662–677. Springer, 2016.
- [35] Yuhao Zhu, Anand Samajdar, Matthew Mattina, and Paul Whatmough. Euphrates: Algorithm-SoC Co-Design for Low-Power Mobile Continuous Vision. In *Proc. of ISCA*, 2018.



# Supplementary Materials

## Proof to Theorem 1

*Proof.* First, it is easy to see that (21) is equivalent to the following problem

$$\max_{\xi \text{ is binary}} \langle Z \odot Z, \xi \rangle, \quad \text{s.t.} \quad \xi \in \Omega(E_{\text{budget}}). \quad (27)$$

Note that if the optimal solution to problem (27) is  $\bar{\xi}$ , the solution to problem (21) can be obtained by  $Z \odot \bar{\xi}$ ; given the solution to (21), the solution to (27) can be obtained similarly.

Therefore, we only need to prove that (27) is equivalent to (23). Meeting the following two conditions guarantees that (27) and (23) are equivalent since they have identical objective functions:

1. Any optimal solution of problem (27) is in the constraint set of problem (23);
2. Any optimal solution of problem (23) is in the constraint set of problem (27).

Let us prove the first condition. Let  $\hat{\xi}$  be the optimal solution to (27). Then for any  $u \in U \cup V$ , the elements of  $Z^{(u)}$  selected by  $\hat{\xi}^{(u)}$  are the largest (in terms of magnitude)  $\|\hat{\xi}^{(u)}\|_0$  elements of  $Z^{(u)}$ ; otherwise there would exist at least one element that can be replaced by another element with a larger magnitude, which would increase the objective value in (27). Since  $\hat{\xi} \in \Omega(E_{\text{budget}})$ , according to the definition of  $A$  in (24),  $\hat{\xi}$  satisfies the constraint of (23).

Let us now prove the second condition. The definition of  $A$  in (24) show that there could at most be two different  $A^{(u)}$  values for each element  $u$ , and the largest  $k$  elements in  $Z^{(u)}$  always have the smaller value, i.e.,  $\alpha_1^{(u)} + \alpha_3^{(u)}$ . Let  $\bar{\xi}$  be the optimal solution to the knapsack problem (23). For any  $u \in U \cup V$ , the elements selected by  $\bar{\xi}^{(u)}$  are also the largest elements in  $Z^{(u)}$  in terms of magnitude; otherwise there would exist an element  $Z_j^{(u)}$  that has a larger magnitude but corresponds to a smaller  $A_j^{(u)}$  ((24) shows that  $A_i^{(u)} \geq A_j^{(u)}$  when  $|Z_i^{(u)}| \leq |Z_j^{(u)}|$ ). This would contradict the fact that  $\bar{\xi}$  is optimal. In addition,  $\bar{\xi}$  meets the constraint in problem (23). Therefore,  $\bar{\xi} \in \Omega(E_{\text{budget}})$ .

It completes the proof.  $\square$

## Proof to Theorem 2

### Problem Formulation

**Definition 1. Inverted knapsack problem.** Given  $n$  objects  $I := \{(v_i, w_i)\}_{i=1}^n$  each with weight  $w_i > 0$ , and value  $v_i \geq 0$ , define  $h_I(x)$  to be the smallest weight budget to have the total value  $x$ :

$$\begin{aligned} h_I(x) &:= \min_{\xi \in \{0,1\}^n} \sum_{i=1}^n w_i \xi_i \\ \text{s. t.} \quad &\sum_{i=1}^n v_i \xi_i \geq x \end{aligned} \quad (28)$$

We are more interested in the case that the weights of  $n$  objects are in  $m$  clusters, i.e. there are only  $m$  distinct weights,

$$|\{w_i\}_{i=1}^n| = m.$$

In our case,  $m$  is proportional to the number of layers in DNN, and  $n$  is the number of all the learnable weights in  $W$ , so  $m \ll n$ .

**Definition 2. Inverse of step function.** *The inverse of the step function  $f$  is defined as the maximal  $x$  having the function value  $y$ :*

$$f^{-1}(y) := \max_{f(x) \leq y} x \quad (29)$$

**Observation** The inverse of the step function  $h_I^{-1}(y)$  is just the maximal value we can get given the weight budget, i.e. the original knapsack problem:

$$h_I^{-1}(y) = \max_{\xi \in \{0,1\}^n} \sum_{i=1}^n v_i \xi_i, \quad \text{s. t.} \quad \sum_{i=1}^n w_i \xi_i \leq y. \quad (30)$$

**Observation** Given a step function with  $l$  breakpoints, its inverse can be generated with  $O(l)$  time complexity, and vice versa.

Thus, given the step function of  $h_I$  in (28) which has  $l$  breakpoints, we can get  $h_I^{-1}$  (i.e. the original knapsack problem) within  $O(l)$  time complexity.

**Definition 3.  $w$ -uniform.** *Step function  $f$  is  $w$ -uniform if the ranges of  $f$  is from  $-\infty, 0, w, 2w, \dots, lw$ .*

**Observation** If all the objects in  $I$  have the same weight  $w$ , i.e.  $m = 1$ , then the function  $h_I(x)$  is nondecreasing and  $w$ -uniform. Moreover, its breakpoints are:

$$(0, 0), (v_1, w), (v_1 + v_2, 2w), \dots, \left( \sum_{i=1}^n v_i, nw \right),$$

if the objects' indices follows the decreasing order in terms of the values, i.e.  $v_1 \geq v_2 \geq \dots \geq v_n$ . Thus we can get all possible function values of  $h_I(x)$ :

$$h_I(x) = kw, \quad \forall x \in \left( \sum_{i=1}^{k-1} v_i, \sum_{i=1}^k v_i \right].$$

**Definition 4. (min, +)-convolution.** *For functions  $f, g$ , the (min, +)-convolution is:*

$$(f \oplus g)(x) = \min_{x'} (f(x') + g(x - x')).$$

**Observation** If object sets  $I_1 \cap I_2 = \emptyset$ , then

$$f_{I_1 \cup I_2} = f_{I_1} \oplus f_{I_2}.$$

**Observation** The inverse of (min, +)-convolution between  $w$ -uniform function  $f$  and  $w$ -uniform function  $g$  is the (max, +)-convolution between  $f^{-1}$  and  $g^{-1}$ :

$$(f \oplus g)^{-1}(y) = \max_{y' \in \{0, 1w, \dots, lw\}} (f^{-1}(y') + g^{-1}(y - y')). \quad (31)$$

**Lemma 4.** *For any  $f$  and  $g$  nonnegative step functions, given an arbitrary number  $b$ , we always have*

$$\min\{f \oplus g, b\} = \min\{\min\{f, b\} \oplus \min\{g, b\}, b\} \quad (32)$$

*Proof.* Given any  $x$ , let  $z \in \text{Arg min}_{x'} f(x') + g(x - x')$  and  $\bar{z} \in \text{Arg min}_{x'} \min(f(x'), b) + \min(g(x - x'), b)$ , so we have  $(f \oplus g)(x) = f(z) + g(x - z)$  and  $(\min\{f, b\} \oplus \min\{g, b\})(x) = \min(f(\bar{z}), b) + \min(g(x - \bar{z}), b)$ .

Consider the following cases:

1.  $(f \oplus g)(x) \geq b$ . In this case, we claim that  $(\min\{f, b\} \oplus \min\{g, b\})(x) \geq b$ . We prove it by contradiction. Suppose  $(\min\{f, b\} \oplus \min\{g, b\})(x) < b$  which implies  $\min(f(\bar{z}), b) + \min(g(x - \bar{z}), b) < b$ . Because both  $f$  and  $g$  are nonnegative, we have  $f(\bar{z}) < b$  and  $g(x - \bar{z}) < b$  which imply  $\min(f(\bar{z}), b) + \min(g(x - \bar{z}), b) = f(\bar{z}) + g(x - \bar{z}) < b$ . However, this contradicts  $(f \oplus g)(x) \geq b$ . Therefore, we have  $\min((f \oplus g)(x), b) = \min((\min\{f, b\} \oplus \min\{g, b\})(x), b) = b$ .
2.  $(f \oplus g)(x) < b$ . In this case, we have  $f(z) < b$  and  $g(x - z) < b$ , so  $\min(f(\bar{z}), b) + \min(g(x - \bar{z}), b) \leq \min(f(z), b) + \min(g(x - z), b) = f(z) + g(x - z) = (f \oplus g)(x) < b$ . Since both  $f$  and  $g$  are nonnegative, we have  $f(\bar{z}) < b$  and  $g(x - \bar{z}) < b$  which imply  $\min(f(\bar{z}), b) + \min(g(x - \bar{z}), b) = f(\bar{z}) + g(x - \bar{z}) \geq (f \oplus g)(x)$ . Therefore, we have  $\min(f(\bar{z}), b) + \min(g(x - \bar{z}), b) = f(\bar{z}) + g(x - \bar{z}) \Leftrightarrow (\min\{f, b\} \oplus \min\{g, b\})(x) = (f \oplus g)(x)$ .

□

### Efficiency of $(\min, +)$ -convolution

**Lemma 5.** *Let  $f$  and  $g$  be nondecreasing  $w$ -uniform functions with  $O(l)$  breakpoints, the  $(\min, +)$ -convolution  $f \oplus g$  (having  $O(l)$  breakpoints) can be generated with  $O(l^2)$  time complexity.*

*Proof.* Firstly, we compute the inverse representation of  $f$  and  $g$ , i.e. compute  $f^{-1}$  and  $g^{-1}$  from Equation (29). The inverse representation can be computed in  $O(l)$  time (proportional to the number of breakpoints). From Equation (31), we can compute the inverse of  $f \oplus g$ . For each  $y \in \{0, 1w, \dots, 2lw\}$ , function  $(f \oplus g)^{-1}(y)$  can be computed in  $O(l)$  time by brute force. Thus a total  $O(l^2)$  is enough to get  $(f \oplus g)^{-1}$  which has  $O(l)$  breakpoints. We can get  $f \oplus g$  via  $(f \oplus g)^{-1}$  by the inverse definition (29) in  $O(l)$  time. □

**Lemma 6.** *Let  $f$  and  $g$  be nondecreasing step functions with  $l$  breakpoints in total,  $\min\{f \oplus g, b\}$  can be approximated by a step function  $\phi_b$  with  $O(l + \frac{1}{\epsilon^2})$  complexity and  $2\epsilon b$  additive error, i.e.  $\min\{f \oplus g, b\} \leq \phi_b \leq \min\{f \oplus g, b\} + 2\epsilon b$ . The resultant function  $\phi_b$  has  $O(1/\epsilon)$  breakpoints.*

*Proof.* We can construct  $(\epsilon b)$ -uniform functions  $f'_b, g'_b$  which have  $\lceil 1/\epsilon \rceil$  breakpoints:

$$f'_b(x) = \left\lceil \frac{\min(b, f(x))}{\epsilon b} \right\rceil \epsilon b, \quad g'_b(x) = \left\lceil \frac{\min(b, g(x))}{\epsilon b} \right\rceil \epsilon b.$$

This needs  $O(l)$  computational complexity. From Lemma 5, we can compute  $f'_b \oplus g'_b$  with  $O(\frac{1}{\epsilon^2})$  time complexity and  $\phi_b = \min\{f'_b \oplus g'_b, b\}$  has  $O(1/\epsilon)$  breakpoints. Because  $f'_b$  and  $g'_b$  are constructed by ceiling  $\min\{f, b\}$  and  $\min\{g, b\}$ , we have:

$$\min\{f, b\} \oplus \min\{g, b\} \leq f'_b \oplus g'_b \leq \min\{f, b\} \oplus \min\{g, b\} + 2\epsilon b,$$

which implies

$$\min\{\min\{f, b\} \oplus \min\{g, b\}, b\} \leq \min\{f'_b \oplus g'_b, b\} \leq \min\{\min\{f, b\} \oplus \min\{g, b\}, b\} + 2\epsilon b.$$

From Lemma 4, we know that  $\min\{\min\{f, b\} \oplus \min\{g, b\}, b\} = \min\{f \oplus g, b\}$ , so it completes the proof. □

**Lemma 7.** Let  $f_1, f_2, \dots, f_m$  be nondecreasing step functions with  $l$  breakpoints in total,  $\min\{f_1 \oplus f_2 \oplus \dots \oplus f_m, b\}$  can be approximated by a step function  $\psi_b$  with  $O(l + m/\epsilon^2)$  computational complexity and  $m\epsilon b$  additive error. The resultant function  $\psi_b$  has  $O(1/\epsilon)$  breakpoints.

*Proof.* From Lemma 6, we have shown the case  $m = 2$ . For general  $m > 2$ , we can construct a binary tree to approximate pairs of functions, e.g., if  $m = 4$ , we can firstly approximate  $\psi^{(1)} \approx \min\{f_1 \oplus f_2, b\}$ , and  $\psi^{(2)} \approx \min\{f_3 \oplus f_4, b\}$ , then approximate  $\psi_b^{(3)} \approx \min\{\psi^{(1)} \oplus \psi^{(2)}, b\}$ .

By this way, we construct a binary tree which has  $O(\log m)$  depth and  $O(m)$  nodes. In the beginning, we use ceil function to construct  $m$  new  $\epsilon b$ -uniform functions:

$$f'_{i,b}(x) = \left\lceil \frac{\min(b, f_i(x))}{\epsilon b} \right\rceil \epsilon b, \forall i \in \{1, 2, \dots, m\}.$$

Then we can use the binary tree to “merge” all the  $m$  functions in pairs, via  $O(\log m)$  iterations. Without loss of generality, we assume  $m$  is a power of two. We can recursively merge  $t$  functions into  $t/2$  functions:

1. Initialize  $t = m$ ,  $g'_{i,b} = f'_{i,b}, \forall i \in \{1, \dots, t\}$ .
2. Reassign  $g'_{i,b} = \min\{g'_{2i-1,b} \oplus g'_{2i,b}, b\}, \forall i \in \{1, \dots, t/2\}$ . According to Lemma 6, the number of break points of  $\min\{g'_{2i-1,b} \oplus g'_{2i,b}, b\}$  is still  $O(1/\epsilon)$ .
3.  $t = t/2$ . If  $t > 1$ , go back to Step 2.
4. Return  $\psi_b := \min\{g'_{1,b}, b\}$ .

For this binary tree, functions of the bottom leaf nodes have  $\epsilon b$  additive error, and every (min, +)-convolution  $f' \oplus g'$  will accumulate the additive error from the two functions  $f'$  and  $g'$ . The root node of the binary tree will accumulate the additive errors from all the  $m$  leaf nodes, thus the resultant function  $\psi_b \leq \min\{f_1 \oplus \dots \oplus f_m, b\} + m\epsilon b$ . For the computational complexity, initializing  $f'_{i,b}$  takes  $O(l)$ , Step 1 takes  $O(l)$ , Step 2 and 3 take  $O(m/\epsilon^2)$  (since there are  $O(m)$  nodes in the binary tree), and Step 4 takes  $O(m/\epsilon)$ . Therefore, there is  $O(l + m/\epsilon^2)$  in total.  $\square$

**Lemma 8.** For the inverted knapsack problem defined in Equation (28), if all the  $n$  objects can be separated into  $m$  groups  $I_1, \dots, I_m$  which have  $m$  distinct weights, there exists an approximate algorithm with computational complexity  $O((n + \frac{m^3}{\epsilon^2}) \log \frac{n \max(w)}{\min(w)})$  which can approximate  $h_I$  by  $\tilde{h}_I$ :

$$h_I(x) \leq \tilde{h}_I(x) \leq (1 + O(\epsilon))h_I(x), \quad \forall x.$$

*Proof.* Firstly, the step function  $h_{I_i}, \forall i \in \{1, 2, \dots, m\}$  can be easily generated within  $O(n \log n)$  by sorting the objects of each group according to their values (in descending order). From the definition of (min, +)-convolution, we know that  $h_I = h_{I_1} \oplus \dots \oplus h_{I_m}$ . Let us construct an algorithm to approximate  $h_I$ :

1. Construct a set  $\mathcal{B} := \{2^i n \max(w) \in [\min(w), n \max(w)]; i \in \mathbb{Z}_{\leq 0}\}$ , where  $\min(w)$  and  $\max(w)$  are the minimum and maximum weight of items respectively, and  $\mathbb{Z}_{\leq 0}$  is the nonpositive integer set. We have  $|\mathcal{B}| = O(\log \frac{n \max(w)}{\min(w)})$ .
2. For every  $b \in \mathcal{B}$ , construct  $\psi_b$  to approximate  $\min\{h_{I_1} \oplus \dots \oplus h_{I_m}, b\}$  based on Lemma 7.

3. Construct function  $\tilde{h}_I^{-1}$ :

$$\tilde{h}_I^{-1}(y) = \begin{cases} \psi_b^{-1}(y), & \text{if } b/2 < y \leq b \text{ and } y > \min(\mathcal{B}); \\ \psi_{\min(\mathcal{B})}^{-1}(y), & \text{if } y \leq \min(\mathcal{B}). \end{cases}$$

where  $\min(\mathcal{B})$  is the minimum element in  $\mathcal{B}$ . The resultant function  $\tilde{h}_I^{-1}$  (or  $\tilde{h}_I$ ) has at most  $O(\frac{1}{\epsilon} \log \frac{n \max(w)}{\min(w)})$  breakpoints.

4. Compute the original function  $\tilde{h}_I$  from  $\tilde{h}_I^{-1}$ .

According to the above procedure, for any  $h_I(x) \in (b/2, b]$ ,  $\tilde{h}_I(x)$  approximate  $h_I(x)$  with additive error  $O(m\epsilon b)$ , so we have  $h_I(x) \leq \tilde{h}_I(x) \leq (1 + O(m\epsilon))h_I(x)$ . The algorithm takes  $O((n + m/\epsilon^2) \log \frac{n \max(w)}{\min(w)})$ , if we require the approximation factor to be  $1 + O(\epsilon)$ , i.e.,

$$h_I(x) \leq \tilde{h}_I(x) \leq (1 + O(\epsilon))h_I(x), \quad \forall x,$$

we need

$$O\left(\left(n + m^3/\epsilon^2\right) \log \frac{n \max(w)}{\min(w)}\right)$$

time complexity. □

**Theorem 9.** *For the knapsack problem defined in Equation (23), if all the  $n$  objects have  $m$  distinct weights, there exists an approximate algorithm with computational complexity  $O((n + \frac{m^3}{\epsilon^2}) \log \frac{n \max(w)}{\min(w)})$  to generate a function  $\tilde{h}_I^{-1}$  satisfying:*

$$h_I^{-1}\left(\frac{y}{1 + O(\epsilon)}\right) \leq \tilde{h}_I^{-1}(y) \leq h_I^{-1}(y), \quad \forall y.$$

*Proof.* From Lemma 8, we have  $\tilde{h}_I(x) \leq (1 + O(\epsilon))h_I(x)$  which implies

$$\{x \mid (1 + O(\epsilon))h_I(x) \leq y\} \subseteq \{x \mid \tilde{h}_I(x) \leq y\}.$$

So

$$\max_{h_I(x) \leq y/(1+O(\epsilon))} x \leq \max_{\tilde{h}_I(x) \leq y} x \Leftrightarrow h_I^{-1}\left(\frac{y}{1 + O(\epsilon)}\right) \leq \tilde{h}_I^{-1}(y).$$

Similarly, we can get  $\{x \mid \tilde{h}_I(x) \leq y\} \subseteq \{x \mid h_I(x) \leq y\}$  from Lemma 8, so we have

$$\max_{h_I(x) \leq y} x \geq \max_{\tilde{h}_I(x) \leq y} x \Leftrightarrow h_I^{-1}(y) \geq \tilde{h}_I^{-1}(y).$$

□

Let  $I$  be the set of objects whose weights are nonzero elements in  $A$  and values are the corresponding elements in  $Z \odot Z$ , i.e.  $I_+ = \{(Z_i^2, A_i) \mid \forall i \in \{1, 2, \dots, |A|\} \text{ and } A_i > 0\}$ ,  $\tilde{\xi}^+$  be the solution corresponding to  $\tilde{h}_I^{-1}(E_{\text{budget}} - \sum_{u \in U \cup V} \alpha_4^{(u)})$ . Let  $\tilde{\xi}_{I_+^c} = \mathbf{1}$  and  $\tilde{\xi}_{I_+} = \tilde{\xi}^+$ , where  $I_+^c = \{(Z_i^2, A_i) \mid \forall i \in \{1, 2, \dots, |A|\} \text{ and } A_i = 0\}$  is the complement of  $I_+$ . Here we have  $m \leq 2|U| + |V|$  distinct values in  $A$ . According to Theorem 9, we have  $\langle Z \odot Z, \tilde{\xi} \rangle \geq \max_{\xi} \langle Z \odot Z, \xi \rangle$ , s.t.  $\langle A, \xi \rangle \leq \frac{E_{\text{budget}} - \sum_{u \in U \cup V} \alpha_4^{(u)}}{1 + O(\epsilon)}$ , which implies

$$\langle Z \odot Z, \tilde{\xi} \rangle \geq \max_{\xi \in \Omega(E_{\text{budget}}/(1+O(\epsilon)))} \langle Z \odot Z, \xi \rangle.$$

From Theorem 9, we can directly get Theorem 2.

### Proof to Theorem 3

*Proof.* From Theorem 1, we know the original projection problem (21) is equivalent to the knapsack problem (23). So proving the inequality (26) is equivalent to proving

$$\langle Z \odot Z, \tilde{\xi} \rangle \geq \langle Z \odot Z, \xi^* \rangle - \text{Top}_{\|\tilde{\xi}\|_0+1}((Z \odot Z) \odot A) \cdot R(\tilde{\xi}) \quad (33)$$

and

$$\langle Z \odot Z, \tilde{\xi} \rangle \geq \langle Z \odot Z, \xi^* \rangle - \text{Top}_{\|\tilde{\xi}\|_0+1}((Z \odot Z) \odot A) \cdot (\max(A) - \gcd(A)), \quad (34)$$

where  $\tilde{\xi}$  is the greedy solution of knapsack problem corresponding to  $W''$ , and  $\xi^*$  is the exact solution of knapsack problem corresponding to  $P_{\Omega(E_{\text{budget}})}(Z)$ , i.e.,

$$W'' = Z \odot \tilde{\xi}, \quad P_{\Omega(E_{\text{budget}})}(Z) = Z \odot \xi^*.$$

Firstly, let us prove the inequality (34). If we relax the values of  $\xi$  to be in the range  $[0, 1]$  instead of  $\{0, 1\}$ , the discrete constraint is removed so that the constraint set becomes

$$\Delta = \left\{ \xi \mid \mathbf{0} \leq \xi \leq \mathbf{1} \text{ and } \langle A, \xi \rangle \leq E_{\text{budget}} - \sum_{u \in U \cup V} \alpha_4^{(u)} \right\}.$$

So the 0/1 knapsack problem is relaxed as a linear programming. This relaxed problem is called fractional knapsack problem, and there is a greedy algorithm [8] which can exactly solve the fractional knapsack problem. Slightly different from our Algorithm 2, the greedy algorithm for the fractional knapsack can select a fraction of the item, so its remaining budget is always zero. The optimal objective value of the fractional knapsack is

$$\max_{\xi \in \Delta} \langle Z \odot Z, \xi \rangle = \langle Z \odot Z, \tilde{\xi} \rangle + \text{Top}_{\|\tilde{\xi}\|_0+1}((Z \odot Z) \odot A) \cdot R(\tilde{\xi}).$$

Since the constraint set of the fractional knapsack problem is a superset of the constraint of the original knapsack problem, we have  $\langle Z \odot Z, \xi^* \rangle \leq \max_{\mathbf{0} \leq \xi \leq \mathbf{1}} \langle Z \odot Z, \xi \rangle$ , that leads to inequality (33).

Secondly, we show that the inequality (34) is also true. Since all the coefficients in  $A$  are multiples of  $\gcd(A)$ , we can relax the original 0/1 knapsack problem in this way: for each item, split them to several items whose coefficients in the constraint are  $\gcd(A)$ , and the coefficients in the objective function are split equally. For the  $j$ -th item, the coefficient in the constraint is  $A_j$  and the coefficient in the objective function is  $(Z \odot Z)_j$ . It will be split into  $A_j/\gcd(A)$  items, and the  $j$ -th item is associated with coefficient  $(Z_j^2/A_j) \cdot \gcd(A)$  in the objective function. This relaxation gives us a new 0/1 knapsack problem, where all the items have the same coefficient in the constraint, so the optimal solution is just selecting the ones with the largest coefficients in the objective function. We can formulate this problem as a relaxed knapsack problem by replacing the constraint of  $\xi$  into  $\xi \in \Gamma$ , where

$$\Gamma = \left\{ \xi \mid \text{for all } j, \xi_j \text{ is a multiple of } \frac{\gcd(A)}{A_j}, 0 \leq \xi_j \leq 1, \text{ and } \langle A, \xi \rangle \leq E_{\text{budget}} - \sum_{u \in U \cup V} \alpha_4^{(u)} \right\}.$$

All the elements of the solution are either 0 or 1 except the last picked one which corresponds to  $\text{Top}_{\|\tilde{\xi}\|_0+1}((Z \odot Z) \odot A)$ . Let the  $(\|\tilde{\xi}\|_0 + 1)$ -th largest element in  $(Z \odot Z) \odot A$  be indexed by  $t$ . We

have  $0 \leq \tilde{\xi}_t \leq 1 - \gcd(A)/A_t$ . Therefore, comparing with the original 0/1 knapsack problem, we have

$$\begin{aligned}
\max_{\xi \in \Gamma} \langle Z \odot Z, \xi \rangle &\leq \langle Z \odot Z, \tilde{\xi} \rangle + (Z \odot Z)_t \cdot (1 - \gcd(A)/A_t) \\
&= \langle Z \odot Z, \tilde{\xi} \rangle + \text{Top}_{\|\tilde{\xi}\|_0+1}((Z \odot Z) \otimes A) \cdot A_t \cdot (1 - \gcd(A)/A_t) \\
&= \langle Z \odot Z, \tilde{\xi} \rangle + \text{Top}_{\|\tilde{\xi}\|_0+1}((Z \odot Z) \otimes A) \cdot (A_t - \gcd(A)) \\
&\leq \langle Z \odot Z, \tilde{\xi} \rangle + \text{Top}_{\|\tilde{\xi}\|_0+1}((Z \odot Z) \otimes A) \cdot (\max(A) - \gcd(A))
\end{aligned}$$

Since  $\{\xi \mid \xi \text{ is binary}\} \subseteq \Gamma$ , we have  $\langle Z \odot Z, \xi^* \rangle \leq \max_{\xi \in \Gamma} \langle Z \odot Z, \xi \rangle$ . So we have the inequality (34).  $\square$